**SPC 01-4065**

# Generation of Very High and Ultrahigh Frequency Broadband Chaotic Signals Using Delay Line Oscillators

**Contract No. F61775-01-WE065**

# FINAL REPORT

# REPORT DOCUMENTATION PAGE

Form Approved OMB No. 0704-0188



| 1. REPORT DATE *(DD-MM-YYYY)* | 2. REPORT TYPE | 3. DATES COVERED *(From – To)* |
|---|---|---|
| 20-08-2002 | Final Report | 19 July 2001 - 19-Jul-02 |

**4. TITLE AND SUBTITLE**

Generation of Very High and Ultrahigh Frequency Broadband Chaotic Signals Using Delay Line Oscillators

**5a. CONTRACT NUMBER**
F61775-01-WE065

**5b. GRANT NUMBER**

**5c. PROGRAM ELEMENT NUMBER**

**6. AUTHOR(S)**

Habil. Dr. Arunas V Tamasevicius

**5d. PROJECT NUMBER**

**5d. TASK NUMBER**

**5e. WORK UNIT NUMBER**

**7. PERFORMING ORGANIZATION NAME(S) AND ADDRESS(ES)**

Semiconductor Physics Institute
A. Gostauto 11
Vilnius LT 2600
Lithuania

**8. PERFORMING ORGANIZATION REPORT NUMBER**

N/A

**9. SPONSORING/MONITORING AGENCY NAME(S) AND ADDRESS(ES)**

EOARD
PSC 802 BOX 14
FPO 09499-0014

**10. SPONSOR/MONITOR'S ACRONYM(S)**

**11. SPONSOR/MONITOR'S REPORT NUMBER(S)**
SPC 01-4065

**12. DISTRIBUTION/AVAILABILITY STATEMENT**

Approved for public release; distribution is unlimited.

**13. SUPPLEMENTARY NOTES**

**14. ABSTRACT**

This report results from a contract tasking Semiconductor Physics Institute as follows: The contractor will investigate chaotic electronic oscillators operating in the VHF and the UHF ranges. Chaos oscillators will be investigated both numerically and experimentally with the goal of developing a systematic approach toward design, active nonlinear device selection, and performance optimization. The research will encompass three aspects in both the VHF frequency range and UHF frequency range:

1. Design of a delay line based oscillator.
2. Development and numerical investigation of the mathematical model.
3. Building and experimental investigation of a hardware prototype.

**15. SUBJECT TERMS**

EOARD, Nonlinear Circuits, Chaotic Circuits, Secure Communications

| 16. SECURITY CLASSIFICATION OF: | | | 17. LIMITATION OF ABSTRACT | 18, NUMBER OF PAGES | 19a. NAME OF RESPONSIBLE PERSON |
|---|---|---|---|---|---|
| a. REPORT | b. ABSTRACT | c. THIS PAGE | | | Christopher Reuter, Ph. D. |
| UNCLAS | UNCLAS | UNCLAS | UL | 26 | 19b. TELEPHONE NUMBER *(Include area code)* +44 (0)20 7514 4474 |

Special contract: **SPC 01-4065**

Contract order No.: **F61775-01-WE065**

Project title: **Generation of Very High and Ultrahigh Frequency Broadband Chaotic Signals Using Delay Line Oscillators**

Period: August 2001 to July 2002

Contractor: Semiconductor Physics Institute,
A. Goštauto 11, Vilnius, LT-2600,
Lithuania
Fax: (3702) 627 123

Number of pages: 26

DATE: July 30, 2002 Signature:
Name and Title of the Principal Investigator: Arūnas Tamaševičius, Habil. Dr.

E-mail: tamasev@uj.pfi.lt

# Contents

Abstract ..... 4
1. Introduction ..... 4
2. Delay line oscillator ..... 6
    2.1. Nonlinear element ..... 6
    2.2. RC low-pass filter ..... 7
    2.3. Amplifier ..... 8
    2.4. Delay line ..... 8
    2.5. Buffer ..... 8
3. Delay differential equations ..... 9
    3.1. Case 1: Single oscillator ..... 9
    3.2. Case 2: Two “slow” oscillators in a ring ..... 10
    3.3. Case 3: “Slow” and “fast” oscillators in a ring ..... 11
    3.4. Numerical results ..... 12
4. Hardware prototypes and experimental results ..... 15
    4.1. “DC” oscillator ..... 15
    4.2. “AC” oscillator ..... 16
    4.3. Improved “AC” oscillator ..... 17
5. Conclusions ..... 20
6. Publications ..... 21
References ..... 22
Disclaimer ..... 24
Declaration ..... 25
Statement ..... 26

## ABSTRACT

The *Final Report* details the research results for the full period from August 2001 to July 2002. It includes a brief overview on chaotic electronic oscillators operating in the RF and the microwave ranges. Special attention is paid to the delay line based chaotic oscillators. The original research contributes to the numerical and experimental investigation of chaotic and hyper-chaotic oscillators for the very high frequency (VHF: 30 to 300 MHz) and the ultrahigh frequency (UHF: 300 to 1000 MHz) ranges. The design of three different versions of a delay line based oscillator, the development, linear analysis and numerical simulation of the appropriate mathematical models, eventually building and experimental investigation of the hardware prototypes are described.


## 1. INTRODUCTION

The first electronic chaos oscillators began to emerge in the late 70s and early 80s. Electronic circuits exhibiting chaotic behavior were rather cheap and relatively easy to build. They were employed as convenient tools for modeling and studying chaotic phenomena, e.g. universal routes to chaos, control of chaos, etc. Meanwhile, electronic chaos oscillators can be readily exploited as high power and high efficiency dynamic noise generators. Another burst of the interest in chaos generators occurred in the early 90s when the American scientists of Naval Research Lab. in Washington, D.C., also of the Massachusetts Institute of Technology suggested an intriguing idea to make use of chaos in secure communications. However, most of the electronic chaos oscillators developed from the 80s were designed and investigated at relatively low frequencies, in the kilohertz range. Only few examples of dynamic chaos generators were developed to operate in the microwave range, e.g. [1-8]. Meanwhile, modern information and military technologies, including computer, radar and communication systems need very high frequency (VHF: 30 to 300 MHz) and ultrahigh frequency (UHF: 300 to 1000 MHz) chaos generators to be developed and used as high power controllable noise sources. For example, in 1996 the Mathematical and Computer Sciences Division, the Electronics Division and the Physics Division of the U.S. Army Research Office (ARO) held an Advanced Concept Workshop "*Communicating by Chaos: Digital Signal Generation by Simple Nonlinear Devices*". One of the conclusions of the Strategic Assessment Report says that "…chaotic oscillators for use as a transmitter at high megahertz to gigahertz frequencies are urgently needed and a better understanding of the physics of nonlinear and active components is required" [9].

Dynamical systems with time delays exhibit very rich dynamics, including high-dimensional hyper-chaotic behavior characterized by multiple positive Lyapunov exponents, broadband continuous spectra, thus can be exploited as noise like signal generators. These systems are commonly presented by the delay differential equations (DDE):

$$\frac{dx(t)}{dt} = F[x(t), x(t-\tau)]. \tag{1.1}$$

Here $x(t)$ is a dynamical variable, $t$ is time, $\tau$ is time delay, and $F[\ldots]$ is a nonlinear function. A specific example of this type of DDE provides the Mackey-Glass (MG) mathematical model [10]:

$$\frac{dx(t)}{dt} = \frac{2x(t-\tau)}{1+x^{10}(t-\tau)} - x(t). \tag{1.2}$$

The first right-hand term in the Eqn.(2) represents a nonlinear function with delay. The MG model has been studied numerically in details by Farmer [11].

To our best knowledge an electronic circuit imitating the MG system has been first described by Dmitriev *et al*. [12]. An acoustic-electric device has been employed for the delay element. Later an analog computer design has been used by Losson *et al*. [13] to simulate the dynamics of a related model – the piecewise constant version of the MG model containing a rectangular nonlinear function. The delay unit in their analog computer has been implemented by means of a sample-and-hold (S&H) chip, or the so-called "bucket brigade device" used along with a clock generator. Actually the computer is a hybrid one containing both time continuous and time discrete units. Later a DDE with a tent type nonlinear function as well as a rectangular one have been considered by Schwarz and Mögel [14]. In addition, the authors of this paper suggested to replace the S&H device by a transmission line (e.g. a coaxial cable), thus yielding a fully time continuous system. Another version of a time continuous delay system has been proposed by Namajūnas *et al.* [15]. Two complementary junction field effect transistors (JFET) coupled in a special way [16] were used to compose the nonlinear device while the delay unit was implemented by means of a high-order L-C-L low-pass filter. The nonlinear device composed of the complementary pair of JFET is described by a function very similar in form to that introduced in the MG model. Therefore, this analog circuit [15] was employed to investigate various features of the hyper-chaotic MG system, including control of chaos/hyperchaos [17,18] and synchronization of chaos/hyperchaos [19-21]. In addition, Pyragas has considered the possibility to apply the MG hyper-chaotic oscillators to secure communications [22].

Most experiments with the MG and related type electronic circuits have been performed at relatively low (kilohertz) frequencies [12,13,15,17-21]. High frequency delay line based chaotic oscillator has been considered by Mögel *et al*. [23]. However, the paper includes only a short note that a practical prototype generates noise like signals in a spectral range from DC to over 100 MHz. Neither details about the nonlinear units nor experimental power spectra are presented in [23].

# 2. DELAY LINE OSCILLATOR

The diagram of a delay line oscillator is sketched in Fig. 1. The oscillator has a ring structure and contains five main units: (1) a nonlinear element **NE**, (2) an **RC** low-pass filter, (3) an amplifier **AMP**, (4) a **Delay line,** and (5) a buffer **BUF.** The latter is an auxiliary unit and may be skipped in some specific designs. The $R_L$ is an external load (commonly 50 Ω).

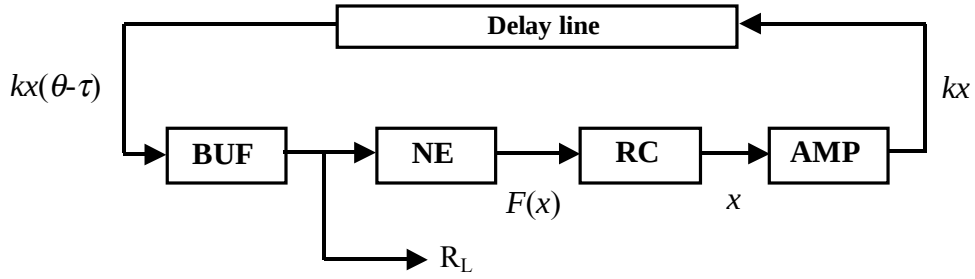


**Fig. 1.** Block diagram of a delay line based oscillator.

## 2.1. Nonlinear element

A simplified circuit diagram of a single transistor Q1 based nonlinear element and its input-output function $V_C$ *vs*. $V_B$ are shown in Fig.2.

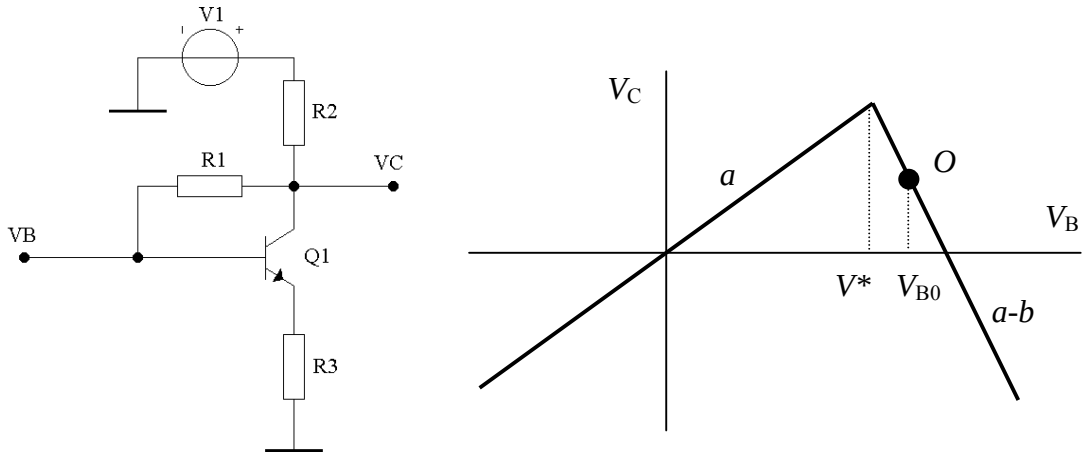


**Fig. 2.** Circuit diagram of the nonlinear element and its input-output function for $b>a$.

The input (base) voltage $V_B$ is a full signal (dc bias $V_{B0}$ + ac signal $V$). The dc component of the output (collector) voltage appearing due to the $V_1$ is removed for simplicity. Thus $V_C$ corresponds to an ac component only. Until $V_B \le V^*$ ($V^*$ is the breakpoint voltage in the current-voltage characteristic of the base-emitter junction; $V^* \approx 0.7$V for silicon transistors) the transistor Q1 is in the OFF-state and the output signal is due to the by-pass resistor R1 only:

$$V_C = \frac{R_2}{R_1 + R_2} V_B = aV_B.$$

When $V_B > V^*$ the Q1 is in the ON-state and

$$V_C = \frac{R_2}{R_1 + R_2} V_B - \frac{R_1 \parallel R_2}{R_3 + r}(V_B - V^*) = aV_B - b(V_B - V^*).$$

Here $R_1 \| R_2$ is the resistance of $R1$ and $R2$ connected in parallel, and $r$ is the small signal resistance of the base-emitter junction of the Q1 in the ON state near the operating point $O$. If $b>a$ the falling segment of the input-output (transfer) function does appear. It is convenient to normalize all the voltages of interest to the breakpoint voltage $V^*$: $V_C/V^*=F$, $V_B/V^*=v$, $V_{B0}/V^*=c$, and $V/V^*=u$. Then the transfer function is given by:

$$F(v) = \begin{cases} av, & v \le 1, \\ (a-b)v + b, & v > 1. \end{cases} \tag{2.1}$$

Since $v=c+u$ the transfer function can be presented in the following form:

$$F\hat{}(u) = \begin{cases} au + ac, & c + u \le 1, \\ (a-b)u + ac - b(c-1), & c + u > 1. \end{cases} \tag{2.1a}$$

Now the operating point $O$ appears on the vertical axis of the plane $[F, u]$. In addition, the operating point $O$ (at $c>1$) can be moved down to the origin by eliminating the constant term $ac-b(c-1)$:

$$F(u) = \begin{cases} au + b(c-1), & c + u \le 1, \\ (a-b)u, & c + u > 1. \end{cases} \tag{2.1b}$$

## 2.2. RC low-pass filter

The 1st-order RC low-pass filter shown in Fig.3.

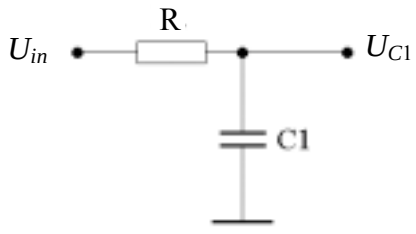


**Fig. 3.** Circuit diagram of the 1st-order RC filter.

Dynamics of the filter is described by the linear ordinary differential equation (ODE):

$$C_1 \frac{dU_{C1}}{dt} = \frac{U_{in} - U_{C1}}{R} \tag{2.2}$$

Here $U_{C1}$ is the voltage across the capacitor C1. Note, that in a specific circuit the output resistance of the previous unit, for example $R_1 \| R_2$ of the nonlinear element may play the role of R. By introducing the dimensionless variables

$$x = \frac{U_{C1}}{V^*}, \quad \theta = \frac{t}{RC_1}, \quad \dot{x} \equiv \frac{dx}{d\theta}$$

and considering the input voltage $U_{in}$ to be just the output voltage the nonlinear element, i.e. $U_{in}=V_C$ Eqn.(2.2) can be given in the following form:

$$\dot{x} = F(u) - x. \tag{2.3}$$

## 2.3. Amplifier

This unit is a linear wideband amplifier with the gain $k$:

$$U_{out} = kU_{in}.$$

Since the input of the amplifier $U_{in}$ is just the output of the RC filter, $U_{in}=U_{C1}$ the normalized output $X=U_{out}/V^*$ is

$$X = kx. \tag{2.4}$$

The amplifier should be a non-inverting one, therefore it should contain an even number of stages (minimum two).

## 2.4. Delay line

Any transmission line, say a segment of 50 Ohm coaxial transmission cable can be used for the delay line (time delay $T_{del}$ is about 5 ns per meter). The end of the transmission line should be loaded with a matched resistor to avoid reflected signals. Taking into account formula (2.4) the normalized delayed signal is given by

$$X_{del} = X(\theta - \tau) = kx(\theta - \tau). \tag{2.5}$$

Here the parameter $\tau$ is a reduced time delay, $\tau = T_{del}/RC_1$.

## 2.5. Buffer

The buffer unit is a simply one- or two-stage emitter follower. Due to its high input impedance it “isolates” the **Delay line** from the nonlinear unit **NE**, thus serves to avoid undesirable loading of the **Delay line**. In addition, because of its low output impedance the external load $R_L$ does not effect the dynamics of the oscillator.

# 3. Delay differential equations

## 3.1. Case 1: Single oscillator

By substituting the indefinite variable $u$ in Eqn.(2.1b) and in the ODE (2.3) with $X_{del}$ from relation (2.5) we obtained a DDE describing the closed-loop (ring) circuit in Fig.1:

$$\dot{x} = F[x(\theta - \tau)] - x. \tag{3.1}$$

Here

$$F = \begin{cases} akx(\theta-\tau) + b(c-1), & c + kx(\theta-\tau) \le 1, \\ (a-b)kx(\theta-\tau), & c + kx(\theta-\tau) > 1. \end{cases} \tag{3.2}$$

The nonlinear function $F$ is depicted for illustration in Fig.4.

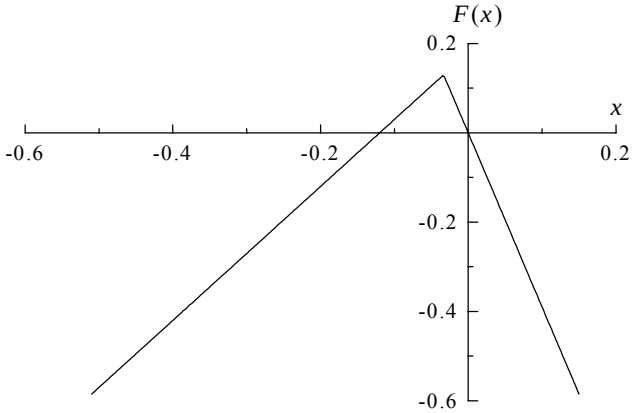


**Fig. 4.** Nonlinear transfer function $F(x)$. $a$=0.5, $b$=1.8, $c$=1.1, $k$=3.

At $\tau$=0 Eqn.(3.1) for $ak$>1 and $b$>$a$ has two different steady state solutions:

$$x_{01} = -\frac{b(c-1)}{ak-1} \qquad \text{and} \qquad x_{02} = 0\,.$$

The $x_{01}$ is an unstable one, while the $x_{02}$ at the origin is a stable one. For non-zero delays Eqn.(3.1) has been solved numerically using the Turbo Pascal software and the Runge-Kutta integration method. At small delays $\tau$<0.49 (for the given parameters) the latter remains stable. At $\tau$>0.49 it turns to be unstable yielding periodic oscillations. In the interval 1.23<$\tau$<1.45 the system undergoes period doubling bifurcations. With further increase of $\tau$ it exhibits chaotic behavior as illustrated in Fig.5.

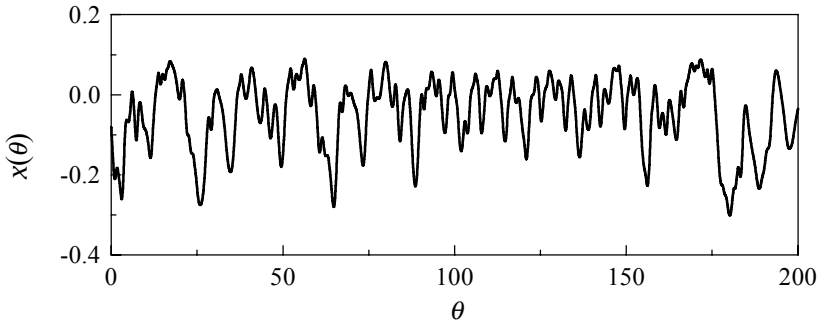


**Fig. 5.** Typical chaotic waveform from Eqn.(3.1). $a$=0.5, $b$=1.8, $c$=1.1, $k$=3, $\tau$=8.

## 3.2. Case 2: Two "slow" oscillators in a ring

Let us consider more complicated case when two oscillators, modules **X** and **Y** each described by Eqn.(3.1) are coupled in a ring as shown in Fig.6. "Slow" oscillators mean that both of them possess the RC low-pass filters in their circuits, that is the C1 in the **X**-module as well as a corresponding capacitor C2 in the **Y**-module have finite non-zero values.

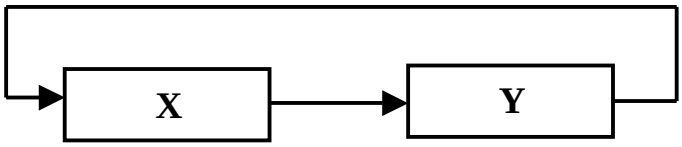


**Fig. 6.** A system of two coupled delay line oscillators.

The coupled system is described by a set of two coupled DDE:

$$\begin{aligned} \dot{x} &= F[y(\theta-\tau_1)]-x, \\ \varepsilon\dot{y} &= F[x(\theta-\tau_2)]-y, \end{aligned} \tag{3.3}$$

with the same type of the nonlinear functions $F(x)$ and $F(y)$ as given by (3.2). In Eqn.(3.3) $\varepsilon=C_2/C_1$, where $C_2$ is the capacitance of the RC filter in the **Y**-module (in general, $C_2\neq C_1$). Numerical analysis shows that two delays $\tau_1$ and $\tau_2$ can be replaced by their sum $\tau=\tau_1+\tau_2$, consequently the set of two DDE is substituted by a simpler set of one DDE and one ODE:

$$\begin{aligned} \dot{x} &= F[y(\theta-\tau)]-x, \\ \varepsilon\dot{y} &= F(x)-y, \end{aligned} \quad \text{or} \quad \begin{aligned} \dot{x} &= F(y)-x, \\ \varepsilon\dot{y} &= F[x(\theta-\tau)]-y, \end{aligned} \tag{3.3a}$$

In (3.3a) both equations, the DDE and the ODE are nonlinear ones. Making use of the fact that in the ring structure any element (at least mathematically) can be moved to any place in the loop the set (3.3) can be further simplified and presented in the form of a nonlinear DDE and a linear ODE:

$$\begin{aligned} \dot{x} &= \Phi[y(\theta-\tau)]-x, \\ \varepsilon\dot{y} &= x-y, \end{aligned} \quad \text{or} \quad \begin{aligned} \dot{x} &= y-x, \\ \varepsilon\dot{y} &= \Phi[x(\theta-\tau)]-y, \end{aligned} \tag{3.3b}$$

Here $\Phi=F\{F[u(\theta-\tau)]\}$, i.e. is a more complicated (double) transfer function of $u$:

$$\Phi=\begin{cases} aF+b(c-1), & c+F\le 1, \\ (a-b)F, & c+F>1. \end{cases} \tag{3.4}$$

The graphical view of $\Phi(x)$ obtained numerically is illustrated in Fig.7. It is a four segment ("double-camel") piecewise linear function. Also an analytic form of $\Phi(x)$ can be derived from (3.2) and (3.4) by means of simple algebra:

$$\Phi=\begin{cases} a^2k^2x+b(c-1)(ak+1), & x\le x_1, \\ a(a-b)k^2x+(a-b)kb(c-1), & x_1\le x\le x_2, \\ (a-b)^2k^2x, & x_2\le x\le x_3, \\ a(a-b)k^2x+b(c-1), & x>x_3, \end{cases} \tag{3.4a}$$

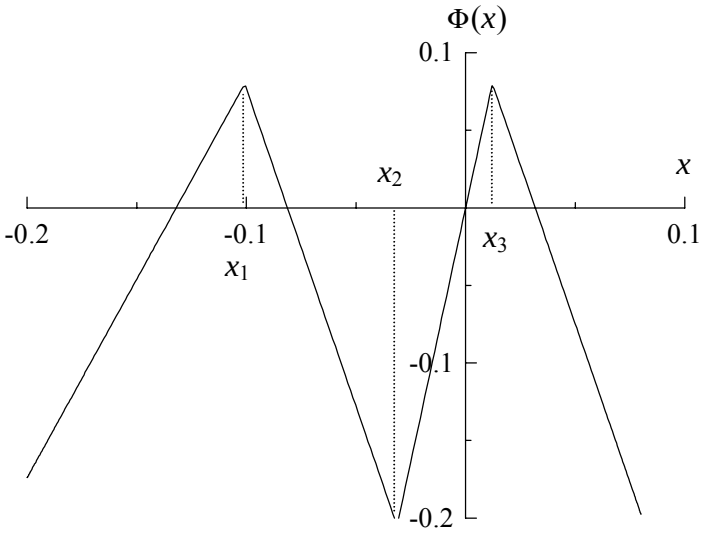


**Fig. 7.** Nonlinear transfer function $\Phi(x)$. $a$=0.5, $b$=1.3, $c$=1.1, $k$=3.2.

where the three break-points are the following:

$$x_1 = -\frac{bk+1}{ak^2}(c-1), \quad x_2 = -\frac{1}{k}(c-1), \quad x_3 = -\frac{1}{(a-b)k^2}(c-1).$$

For the given parameter values $x_1$, $x_2$<0 and $x_3$>0 ($a$<$b$) in agreement with the graph in Fig.7.

## 3.3. Case 3: "Slow" and "fast" oscillators in a ring

In the limit when $\varepsilon$=0 ($C_2$=0), that is the second oscillator is "fast" we come back to a single DDE similar to Eqn.(3.1) for the Case 1 but with a different nonlinear function :

$$\dot{x} = \Phi[x(\theta - \tau)] - x. \tag{3.5}$$

At $\tau$=0 Eqn.(3.5), with $\Phi(x)$ described by (3.4 or 3.4a) has four different steady state solutions:

$$x_{01} = -\frac{b(c-1)}{ak-1}, \quad x_{02} = -\frac{(a-b)kb(c-1)}{a(a-b)k^2-1}, \quad x_{03} = 0, \quad \text{and} \quad x_{04} = -\frac{b(c-1)}{a(a-b)k^2-1}.$$

The $x_{01}$ and the $x_{03}$ are exactly the same as the $x_{01}$ and the $x_{02}$ in the **Case 1** of the two segment function $F(x)$. However, in contrast to the **Case 1** they are both unstable solutions, including $x_{03}$ at the origin, because they appear on the raising segments of $\Phi(x)$. Meanwhile another pair of the steady state solutions, $x_{02}$ and $x_{04}$ that appear on the falling segments of the transfer function are stable ones. Similarly to the **Case 1** they become unstable for non-zero delays.

The steady state analysis performed here at $\tau$=0 for the **Case 3** can be useful for the **Case 2** as well, since four values of the steady state solutions, $x_{0i}$ (i=1,.., 4) are identical ones in both cases. While another four values, $y_{0i}$ are obtained immediately: $y_{0i}$=$F(x_{0i})$ for Eqn.(3.3 or 3.3a) and $y_{0i}$=$x_{0i}$ for Eqn.(3.3b).

## 3.4. Numerical results

In this section the qualitative and quantitative numerical results for all the three discussed cases are presented. The results include phase portraits, Poincaré sections, Lyapunov exponents, Kolmogorov entropy and power spectra.

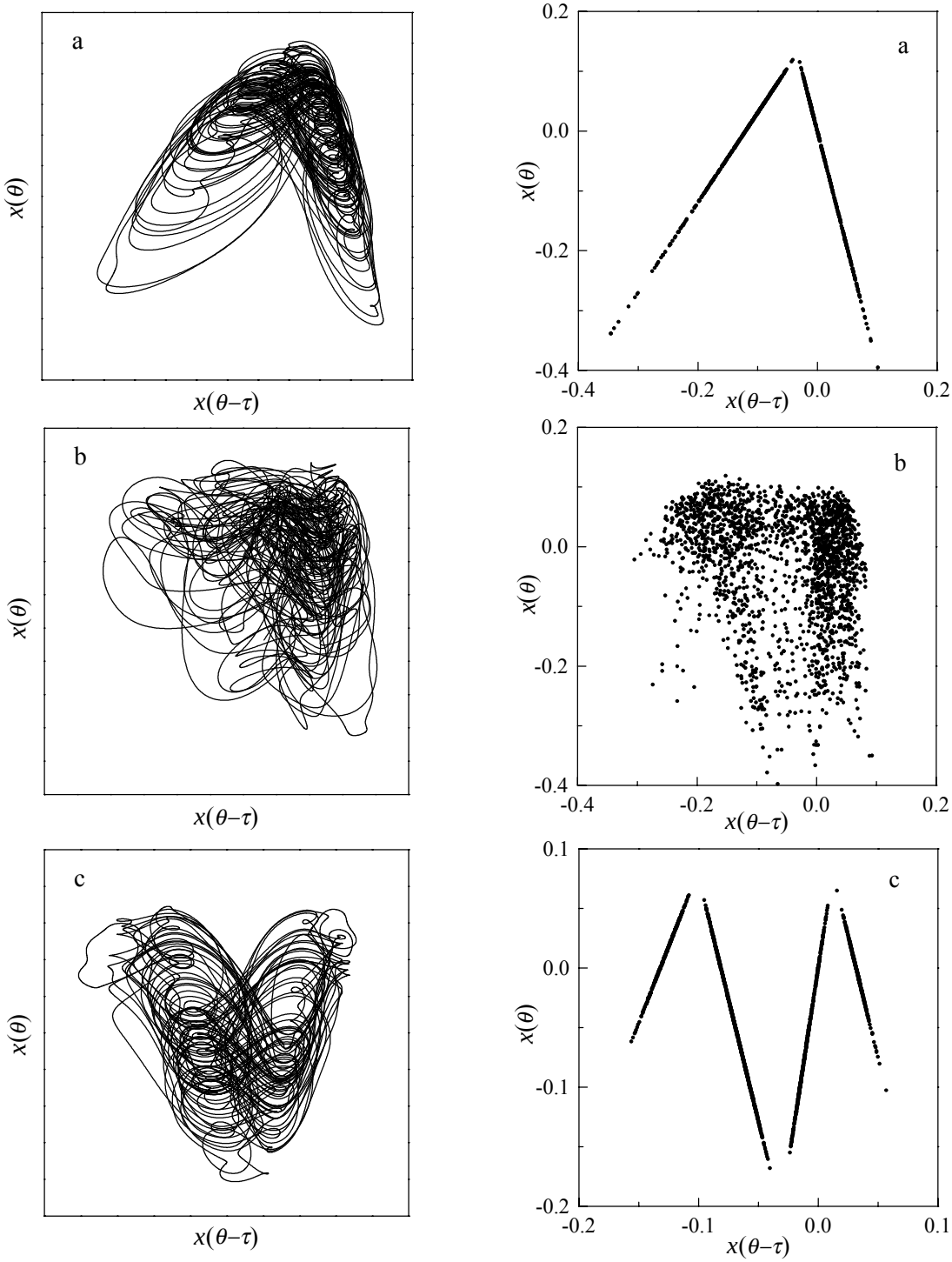


**Fig. 8.** Phase portraits (left) and Poincaré sections (right) in three different cases:
(a) case 1 from Eqn.(3.1). $a$=0.5, $b$=1.8, $c$=1.1, $k$=3, $\tau$=8.
(b) case 2 from Eqn.(3.3a). $a$=0.5, $b$=1.8, $c$=1.1, $k$=3, $\tau$= 8, $\varepsilon$=1.
(c) case 3 from Eqn.(3.5). $a$=0.5, $b$=1.3, $c$=1.1, $k$=3.2, $\tau$=8, ($\varepsilon$=0).
The Poincaré sections are taken at the local maxima of the $x(t)$, that is at $dx/dt$=0.

One can see that the phase portraits in Case 2 and Case 3 are more complicated than in Case 1, that is similar, as expected, to the phase portrait of the MG system [11,15]. An interesting fact, that the Poincaré sections in Case 1 and Case 3 are linear (one-dimensional) ones. Moreover, they do coincide with the transfer functions $F(x)$ in Fig.4 and with $\Phi(x)$ in Fig.7, respectively. However, this is not an unexpected feature. It comes in a straightforward way from Eqn.(3.1) and Eqn.(3.5). Indeed, if we set the Poincaré condition $dx/dt=0$, then $x=F[x(\theta-\tau)]$ and $x=\Phi[x(\theta-\tau)]$ in the Case 1 and Case 3, respectively. Meanwhile the dots of the Poincaré section in the Case 2 is scattered in the plane, that is an essentially two-dimensional one.

In addition, all the three cases have been characterized quantitatively by the Lyapunov exponents (LE) (Fig.9). In Case 1 the system becomes chaotic (has one positive LE) at $\tau=1.5$ as discussed above on page 9. With the increase of $\tau$ more and more positive LE do appear, that is the system becomes a hyper-chaotic one. Similar behavior is observed in Case 2 and Case 3. The difference is in the fact, that chaos emerges at lower delays ($\tau=1$) and the values of the LE are nearly twice larger.

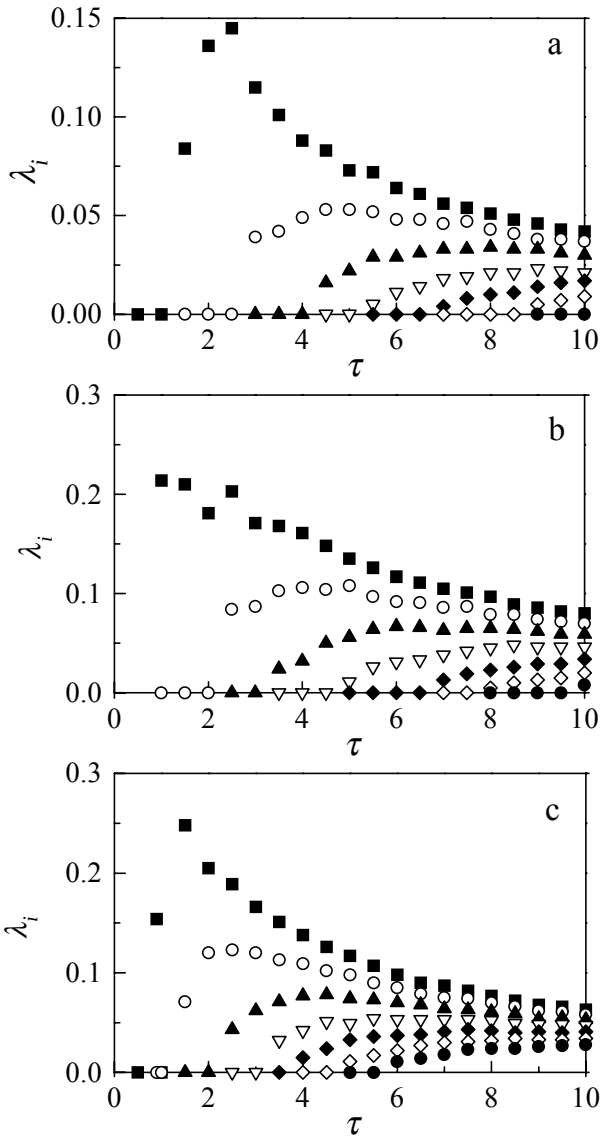


**Fig. 9.** Non-negative Lyapunov exponents $\lambda_i$ *versus* the delay $\tau$ in three different cases: (a) case 1, (b) case 2, (c) case 3. Parameters are the same as in Fig.8.

The results of Fig.9 are summarized in Fig.10, where the number of positive LEs $n^+$ and the Kolmogor entropy, i.e. the sum of the positive LE: $H=\Sigma\lambda^+$ are presented.

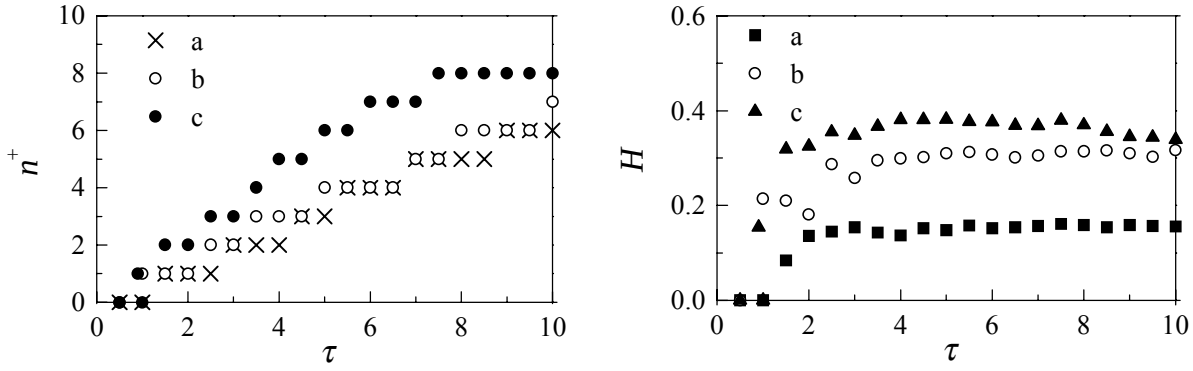


**Fig. 10.** Number of positive Lyapunov exponents (left) and the Kolmogorov entropy (right). The letters a, b, and c in the legends correspond to the cases of Fig.9.

Finally, we present in Fig.11 the power spectra simulated from the variable $x(t)$. One can see that the most smooth spectrum is in the Case 2.

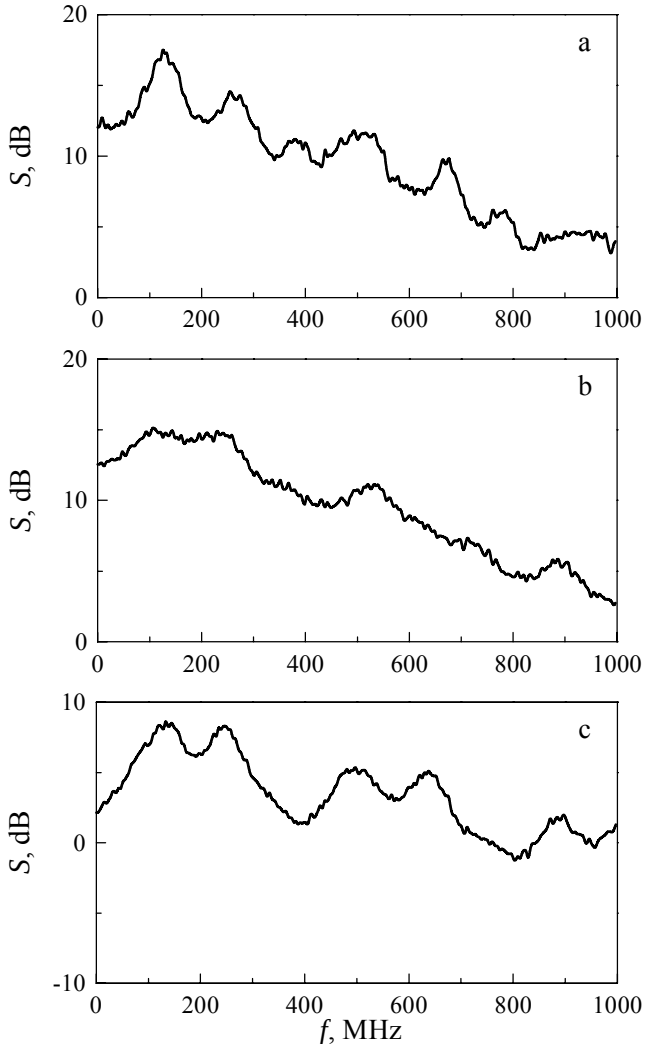


**Fig. 11.** Simulated power spectra for three different cases:
(a) case 1, (b) case 2, (c) case 3. Parameters are the same as in Fig.8.

# 4. Hardware prototypes and experimental results

We have developed three practical modifications of the delay line based chaotic oscillator: (*i*) a "DC" one with the bandwidth of its units from dc to several gigahertz, (*ii*) a broadband "AC" one with the bandwidth of its units from several megahertz to several gigahertz, and (*iii*) an impoved version of the "AC" oscillator having better stability and reproducibility.

## 4.1. "DC" oscillator

The first version of the experimental chaotic oscillator, the "DC" one without blocking capacitors between the stages is presented in Fig.12.

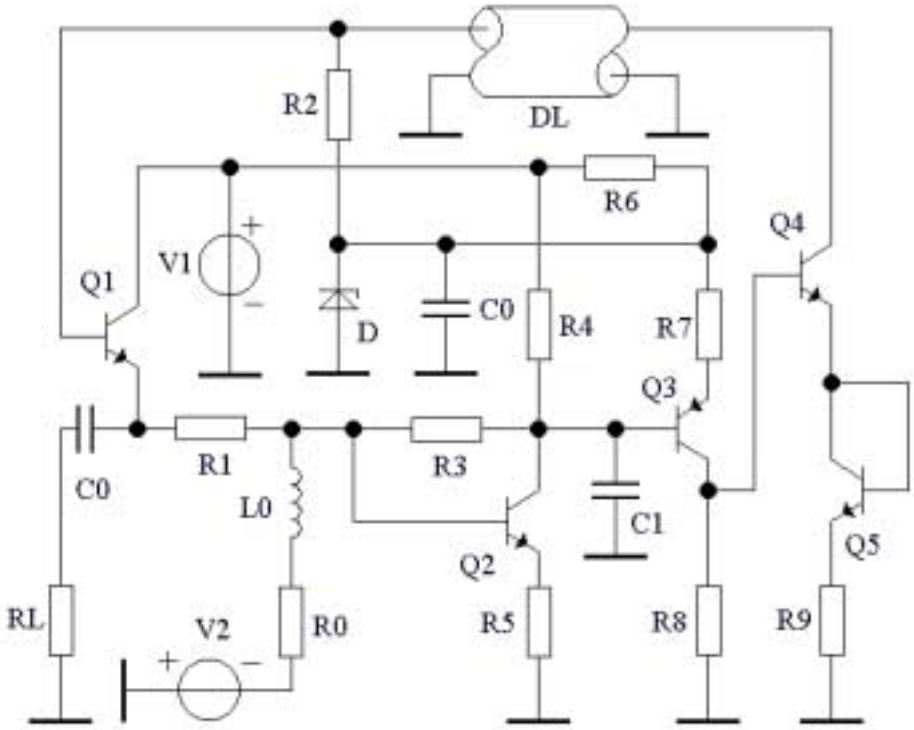


**Fig. 12.** Circuit diagram of the "DC" chaotic oscillator (one module).

The Q1-stage is a buffer and the Q2-stage is a nonlinear unit. The output resistance of the latter is formed by the (R1+R3) and R4 in parallel. The linear non-inverting amplifier is based on Q3 and Q4. We note, that in order match the dc biases between the subsequent stages a *p-n-p* transistor is exploited for Q3, while all the other transistors are *n-p-n* type ones. The delay line DL (a coaxial transmission cable of length L) is coupled to the matched resistor R2. The C0 in series with the external load RL is a blocking capacitor, while C0 in parallel with the Zener diode D is a filtering one. The diode D, the auxiliary transistor Q5, the voltage source V2, and the resistors R0 and R6 serve to set appropriate dc biases of the transistors. The L0 is a choke used to block ac signals.

The specific circuit parameters are the following: $R_0$=$R_1$=$R_2$=$R_8$=51 Ω, $R_3$=$R_4$=75 Ω, $R_5$=11 Ω, $R_6$=$R_9$=16 Ω, $R_7$=33 Ω, $C_0$=47 nF, $C_1$=8 pF, $L_0$=4 μH, L=40 cm (the RG58U type coaxial cable; time delay is ≈ 5 ns/m; $T_{del}$ ≈ 2 ns), $V_1$=8 V, V2=4.5 to 5.5 V. The Q1, Q1, Q2,

Q4, and Q5 are the BFG520 *n-p-n* type transistors ($f_{th}$=9 GHz), Q3 is the BFR194 *p-n-p* one ($f_{th}$=5 GHz). The D is the BZV55-C6V2 or similar type Zener device. In the RC filter $R=R_4\|(R_1+R_3)$= 47 Ω, thus the time constant $RC_1 \approx 0.4$ ns. Taking into account the time lag in the circuit itself the total delay time $T_{del} \approx 2.3$ ns, and the dimensionless delay parameter $\tau = T_{del}/RC_1 \approx 6$. Power spectra of this "DC" hardware prototype are presented in Fig.13.

The "DC" oscillators when coupled in a ring structure exhibit noticeably smoother power spectrum than a single (one module) oscillator (Fig.13b compared with Fig.13a).

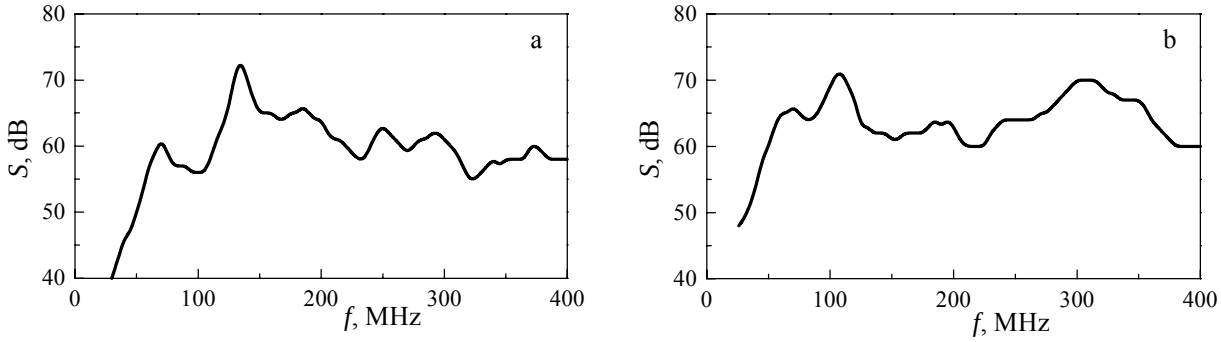


**Fig. 13.** Experimental power spectra from the "DC" chaotic oscillator. $V_1$=8 V and $V_2$=5 V. (a) single module, (b) two modules in a ring (L1+L2=L=40 cm, $C_2=C_1$). Spectral resolution $\Delta f$=120 kHz. The level of 0dB corresponds to 1 μV across 50 Ω load.

## 4.2. "AC" oscillator

The circuitry of the "AC" oscillator containing blocking capacitors between the stages is shown in Fig.14.

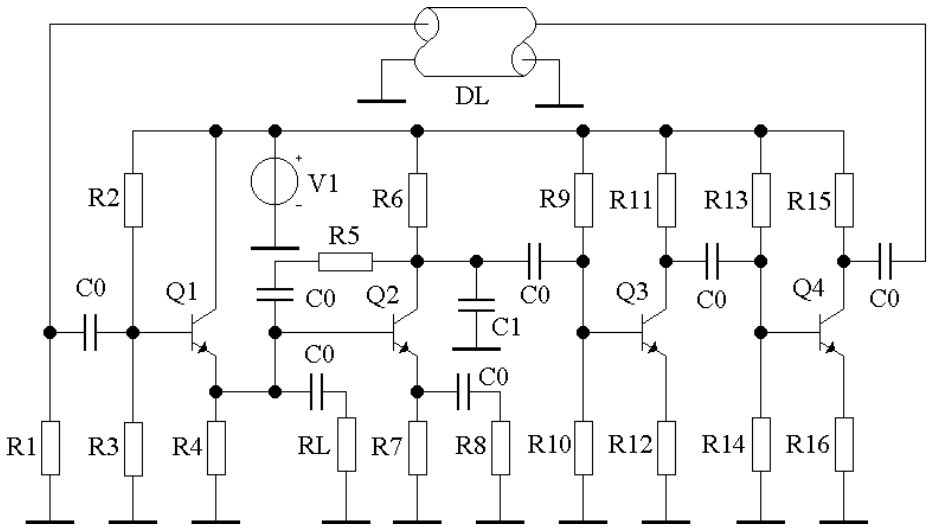


**Fig. 14.** Circuit diagram of the "AC" chaotic oscillator (one module).

The emitter follower (Q1-stage) is a buffer. Low dc biased (2 to 3 mA) Q2-stage plays the role of a nonlinear unit. The output resistance of the nonlinear unit R5||R6 together with the capacitor C1 compose the low-pass RC filter. Two-stage circuit (Q3-Q4) is a non-inverting linear amplifier. The delay line DL is simply a length L segment of a coaxial transmission cable. It is coupled to the matched resistors R1 and R15. The C0 are the blocking capacitors. The RL is an external load, e.g. an input of a measuring device, power amplifier, etc. Due to low output impedance of the buffer the oscillator is not sensitive to RL.

In a specific circuit the parameters are as follows: $R_1$=$R_5$=$R_6$=$R_{11}$=$R_{15}$=51 Ω, $R_2$=2.7 kΩ, $R_3$=4.7 kΩ, $R_4$=150 Ω, $R_7$=680 Ω, $R_8$=10 Ω, $R_9$=$R_{13}$=4.7 kΩ, $R_{10}$=$R_{14}$=1.5 kΩ, $R_{12}$=$R_{16}$=16 Ω, $C_0$=47 nF, $C_1$=12 pF, L=40 cm (RG58U type coaxial cable; time delay is ≈ 5 ns/m; $T_{del}$ ≈ 2 ns), $V_1$=5 to 6 V. The transistors Q1 to Q4 are the BFG520 *n-p-n* type silicon devices ($f_{th}$=9 GHz). In the RC filter $R$=$R_5$||$R_6$=25 Ω, thus the time constant $RC_1$≈0.3 ns (the parasitic collector-base capacitance of Q1 is small compared with $C_1$). Taking into account time lag in the circuit itself the total delay time $T_{del}$ ≈ 2.3 ns, and the dimensionless delay parameter $\tau$ =$T_{del}$/$RC_1$ ≈ 8. Power spectra of the hardware prototype are presented in Fig.15.

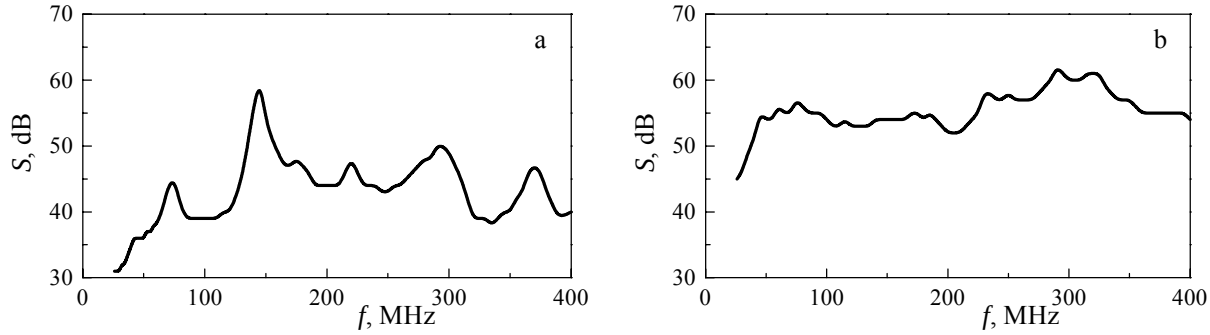


**Fig. 15.** Experimental power spectra from the "AC" oscillator. $V_1$=5.4 V
(a) single module, (b) two modules in a ring (L1+L2=L=40 cm, $C_2$=$C_1$)
Spectral resolution Δ$f$=120 kHz. The level of 0dB corresponds to 1 μV across 50 Ω load.

One can see in Fig.15 that the power spectrum in the case of two coupled modules is much smoother than in the case of a single module (Fig.15b compared with Fig.15a). This experimental observation is in a good agreement with numerical prediction (Fig.11a,b).

Meanwhile there is no much difference in the power spectra of the "AC" and the "DC" oscillators in the single/two module cases (see Fig.15a and Fig.13a, Fig.15b and Fig.13b).

## 4.3. Improved "AC" oscillator

The circuit of the improved "AC" oscillator stages is presented in Fig.16.

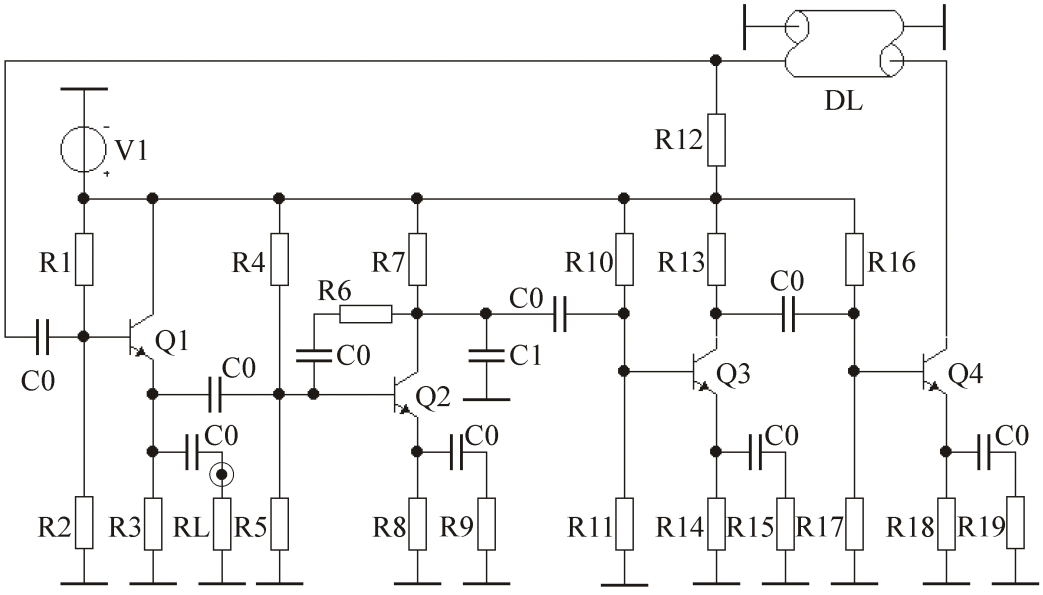


**Fig. 16.** Circuit diagram of the improved "AC" chaotic oscillator (one module).

The role of the stages based on Q1, Q2, and Q3–Q4 in Fig.16 is the same as in the previous "AC" circuit shown in Fig.14. The main circuitry differences are the following:

(1) The buffer (Q1-stage) and the nonlinear element (Q2-stage) are separated by means of the blocking capacitor C0. The Q2 has its own dc bias voltage divider R4/R5. Though this modification requires some additional circuit elements it allows one to set the operating point of the nonlinear element independently of the buffer settings.

(2) In the amplifier (Q3–Q4-stages) large resistors R14 and R18 are inserted in the emitter loops to stabilize the dc conditions of the transistors. Meanwhile the ac gain of the stages depend mainly on of small resistors R15 and R19 (strictly speaking on the parallel chains R14||R15 and R18||R19).

(3) In contract to the circuit in Fig.14 the output stage of the amplifier (Q4-stage) in Fig.16 is loaded directly with the DL, the other end of which is loaded with a matching resistor R12. This solution enables one to increase the gain of the stage by a factor of 2 in comparison with the amplifier in Fig.14 or to have the same gain but with a twice larger resistor R18||R19 in the emitter loop of the transistor Q4. The larger values of R18||R19 do stabilize the gain value of the stage.

In a specific oscillator the circuit parameters are the following: $R_1$=$R_{10}$=$R_{16}$=6.8 kΩ, $R_2$=$R_5$=$R_{11}$=$R_{17}$=2.7 kΩ, $R_3$=$R_8$=$R_{14}$=$R_{18}$=100 Ω, $R_4$=18 kΩ, $R_6$=$R_7$=$R_{12}$=$R_{13}$=51 Ω, $R_9$=11 Ω, $R_{15}$=$R_{19}$=33 Ω, $C_0$=47 nF, $C_1$=12 pF to 5.6 pF, L=40 cm to 10 cm (RG58U type coaxial cable, time delay is ≈ 5 ns/m, $T_{del}$ ≈ 2 to 0.5 ns), $V_1$=8 to 9 V. The transistors Q1 to Q4 are the BFG520 *n-p-n* type silicon devices ($f_{th}$=9 GHz). In the RC filter $R$=$R_6$||$R_7$=25 Ω, thus the time constant $RC_1$ ≈ 0.3 ns to 0.14 ns (the parasitic collector-base capacitance of Q2 is small compared with $C_1$). The time lag in the circuit itself is about 0.3 ns, thus the total delay time $T_{del}$ ≈ 2.3 ns to 0.8 ns for L=40 cm and L=10 cm, respectively. Correspondingly, the dimensionless delay parameter $\tau = T_{del}/RC_1 \approx 8$ at {$C_1$=12 pF, L=40 cm), and $\tau = T_{del}/RC_1 \approx 6$ at {$C_1$=5.6 pF, L=10 cm).

Power spectra of this hardware prototype for different values of the capacitances $C_1$, $C_2$ and different lengths L of the delay line are presented in Fig.17 and Fig.18.

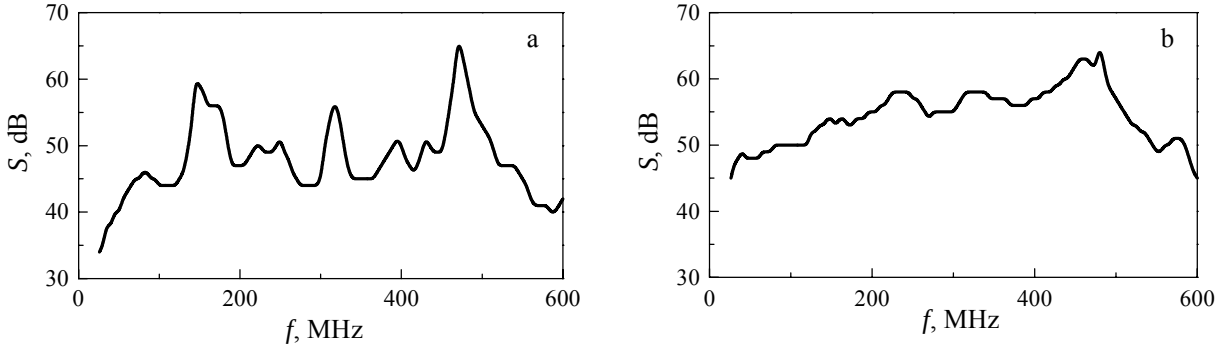


**Fig. 17.** Experimental power spectra from the improved oscillator.
(a) single module ($C_1$=12 pF, L=40 cm, $V_1$=8.3 V),
(b) two modules in a ring (L1+L2=L=40 cm, $C_2$=$C_1$, $V_1$=8.8 V)
Spectral resolution Δ$f$=120 kHz. The level of 0 dB corresponds to 1 μV across 50 Ω load.

One can see here again that the power spectrum from two-module oscillator (Fig.17b) is considerably smoother than that from the single-module oscillator. The unevenness of the spectrum is about 10 dB in the frequency range 30 to 400 MHz that covers the VHF band.

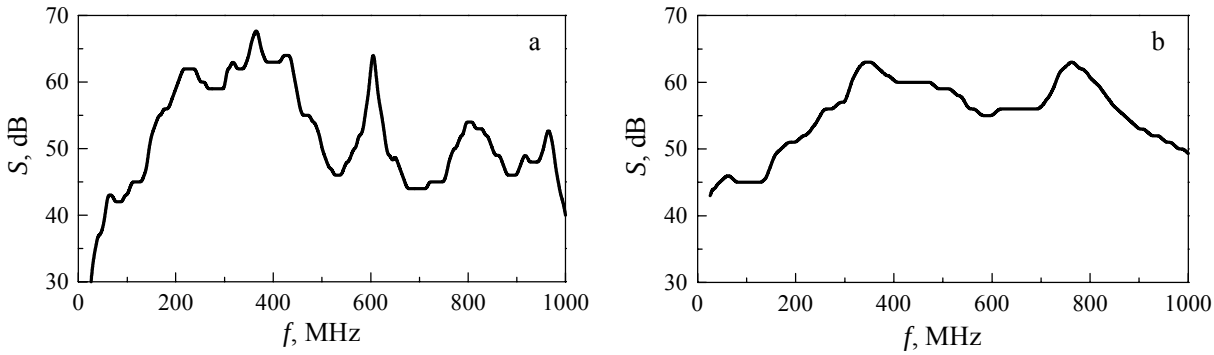


**Fig. 18.** Experimental power spectra from the improved oscillator.
(a) single module ($C_1$=5.6 pF, L=10 cm, $V_1$=8.8 V),
(b) two modules in a ring (L1+L2=L=10 cm, $C_2$=$C_1$, $V_1$=8.8 V)
Spectral resolution $\Delta f$=120 kHz. The level of 0 dB corresponds to 1 μV across 50 Ω load.

The two-module oscillator with $C_1$=$C_2$=5.6 pF and L=10 cm exhibits rather smooth power spectrum (Fig.18b). The unevenness of the spectral density is about 10 dB in the UHF (300 to 1000 MHz) range.

# 5. CONCLUSIONS

1. The developed delay line based oscillators at the time delays $\tau \geq 1.5$ generate chaotic signals. At larger delays, $\tau \geq 3$ they exhibit hyper-chaotic behavior characterized by multiple positive Lyapunov exponents.
2. Two oscillators coupled in a ring (two-module oscillators) have larger positive Lyapunov exponents, higher Kolmogorov entropy, more complicated two-dimensional structure of the Poincaré sections and provide essentially smoother power spectra than a single oscillator.
3. The hardware prototypes generate powerful broadband chaotic oscillations in the very high frequency (VHF: 30 to 300 MHz) and the ultrahigh frequency (UHF: 300 to 1000 MHz) ranges. The unevenness of the spectral density is about 10 dB in the case of two-module oscillators.
4. Though the "DC" circuit has larger bandwidths of the units there is no essential difference between the results of the "DC" and the "AC" chaotic oscillators. The "DC" version contains less circuit elements than the "AC" one. However, in the "DC" oscillator it is much more difficult to set the appropriate dc biases and to couple neighboring dc units. In addition, the "DC" modification uses the *p-n-p* type silicon transistors that commonly have lower threshold frequencies $f_{th}$ than the *n-p-n* ones. Consequently, the "AC" chaotic oscillators have an advantage over the "DC" ones.
5. Further research could be focused on the possibilities to increase the fundamental frequency of chaotic and hyper-chaotic oscillations, that is to move or extend the power spectra to the *S*-band (1 to 2 GHz) of the microwave range. The solutions could involve different modifications of both the delay line oscillator and the Colpitts oscillator, individual ones as well as the oscillators coupled in arrays.

# 6. PUBLICATIONS

The following International conference proceedings and *journal* papers include an acknowledgment of the Government's support:


1. A. Čenys, E. Lindberg, A. N. Anagnostopoulos, G. Mykolaitis, and A. Tamaševičius. Broadband hyperchaotic oscillator with delay line, in: Experimental Chaos: Proc. 6th Experimental Chaos Conference, ECC6. - World Scientific, Singapore, 2002.
2. S. Bumelienė, G. Mykolaitis, G. Lasienė, A. Čenys, and A. Tamaševičius. Evaluation of high speed bipolar transistors for application to chaotic Colpitts oscillator, in: Ultrafast Phenomena in Semiconductors, S.Ašmontas, A.Dargys, H.G.Roskos, Eds. (Trans. Tech. Publ. Ltd.), *Material Science Forum*, 2001, v. 384-385, p. 151-154.
3. A. Tamaševičius, S. Bumelienė, and G. Mykolaitis. Evaluation of bipolar transistors for application to RF chaotic Colpitts oscillator, *Scientific Proceedings of Riga Technical University, ser 7, Telecommunications and Electronics*, 2001, v. 1, p. 53-54.
4. A. Baziliauskas, A. Tamaševičius, S. Bumelienė, and E. Lindberg. Synchronization of chaotic Colpitts oscillators, *Scientific Proceedings of Riga Technical University, ser 7, Telecommunications and Electronics*, 2001, v. 1, p. 55-58.
5. G. Mykolaitis, A. Čenys, S. Bumelienė, and A. Tamaševičius. VHF and HF hyperchaotic oscillators with delay line, in: Proc. 10th Int. Workshop on Nonlinear Dynamics of Electronic Systems, NDES'2002, Izmir Institute of Technology, Izmir Turkey, p. 2/33-2/36.
6. A. Tamaševičius, A. Čenys, A. Baziliauskas, R. Krivickas, and E. Lindberg. Hyperchaotic behavior of weakly coupled Colpitts oscillators, in: Proc. 10th Int. Workshop on Nonlinear Dynamics of Electronic Systems, NDES'2002, Izmir Institute of Technology, Izmir Turkey, p. 4/13-4/16.
7. A. Tamaševičius, G. Mykolaitis, A. Čenys, and S. Bumelienė. Two delay line hyperchaotic oscillators in a ring, in: Experimental Chaos: Proc. 7th Experimental Chaos Conference, ECC7, accepted.
8. A. Čenys, A. Tamaševičius, G. Mykolaitis, and S. Bumelienė. Coupled VHF delay line chaos generators, in: Proc. 1st Int. Workshop on Noise Radar Technology, NRTW-2002, Yalta, Ukraine, accepted.

# REFERENCES


[1] Yu. F. Shirokov and A. I. Kolpakov. Powerful generator of narrow-band noise, Pribory i tekhnika eksperimenta, 1986, No. 2, p. 123-124 (in Russian).

[2] A. Namajūnas and A. Tamaševičius. Application of gallium arsenide tunnel diodes for generation of microwave noise, Elektronnaja Tekhnika, ser. 2, 1990, No. 1(204), p. 69-72 (in Russian).

[3] C. Wegener and M. P. Kennedy. RF chaotic Colpitts oscillator, in: Proc. 3rd Int. Workshop on Nonlinear Dynamics of Electronic Systems, NDES'95, Dublin, Ireland, p. 255-258.

[4] M. I. Sobhy and A. R. Shehata. Chaotic J-band generator for radar and microwave communication systems, in: Proc. 29th European Microwave Conference, 1999, Munich, Germany, p. 202-205.

[5] A. Panas, B. Kyarginsky, and N. Maximov. Single-transistor microwave chaotic oscillator, in: Proc. Int. Symp. on Nonlinear Theory and its Applications, NOLTA'2000, Dresden, Germany, p. 445-448.

[6] A. Tamaševičius *et al*. Two-stage chaotic Colpitts oscillator, Electronics Letters, 2001, v. 37, No. 9, p. 549-551.

[7] G. Mykolaitis *et al*. Towards microwave chaos with two-stage Colpitts oscillator, in: Proc. 9th Int. Workshop on Nonlinear Dynamics of Electronic Systems, NDES'2001, Delft, the Netherlands, p. 97-100.

[8] A. Tamaševičius *et al*. Synchronization of VHF chaotic Colpitts oscillators, in: Proc. 9th Int. Workshop on Nonlinear Dynamics of Electronic Systems NDES'2001, Delft, the Netherlands, p. 223-226.

[9] Toward a New Digital Communication Technology Based on Nonlinear Dynamics and Chaos: Strategic Assessment Report, Mathematical and Computer Science Division**,** U.S. Army Research Office, 1996.

[10] M. C. Mackey and L. Glass. Oscillation and chaos in physiological control system, Science, 1997, v. 197, No. 4300, p. 287-289.

[11] J. D. Farmer. Chaotic attractor of an infinite-dimensional dynamical system, Physica D, 1982, v. 4, No. 3, p. 366-393.

[12] A. S. Dmitriev, Yu. N. Orlov, and S. O. Starkov. Estimation of strange attractors dimensions in the ring self-generator with delay line, Radiotekhnika i elektronika, 1989, v. 34, No. 9, p. 1980-1983, in Russian.

[13] J. Losson, M. C. Mackey, and A. Longtin. Solution multistability in first-order nonlinear differential delay equations, Chaos, 1993, v. 3, No. 1, p. 167-176.

[14] W. Schwarz and A. Mögel. Chaos generators with transmission line, in: Proc. 2nd Int. Workshop on Nonlinear Dynamics of Electronic Systems, NDES'94, Krakow, Poland, p. 239-244.

[15] A. Namajūnas, K. Pyragas, and A. Tamaševičius. An electronic analog of the Mackey-Glass system, Physics Letters A, 1995, v. 201, No. 1, p. 42-46.

[16] L. O. Chua, J. Yu, and Y. Yu. Bipolar-JFET-MOSFET negative resistance devices, IEEE Trans. Circuits and Systems I, 1985, v. 32, No. 1, p. 46-61.

[17] A. Namajūnas, K. Pyragas, and A. Tamaševičius. Stabilization of an unstable steady state in a Mackey-Glass system, Physics Letters A, 1995, v. 204, No. 2, p. 255-262 .

[18] A. Namajūnas, K. Pyragas, and A. Tamaševičius. Analog techniques for modeling and controlling the Mackey-Glass system, Int. J. Bifurcation and Chaos, 1997, v. 7, No. 4, p. 957-962.

[19] A. Tamaševičius *et al*. Synchronization of hyperchaotic oscillators, Electronics Letters, 1997, v. 33, No. 7, p. 2025-2026.
[20] A. Tamaševičius *et al*. Synchronizing hyperchaotic circuits, in: Applied Nonlinear Dynamics and Stochastic Systems near the Millennium, J. B. Kadtke and A. Bulsara, Eds., AIP Conference Proceedings vol.411, New York: American Institute of Physics, 1997, p. 81-86.
[21] A. Tamaševičius *et al*. Synchronizing hyperchaos in infinite dimensional dynamical systems, Chaos, Solitons & Fractals, 1998, v. 9, No. 8, p. 1403-1408.
[22] K. Pyragas. Transmission of signals via synchronization of chaotic time-delay systems, Int. J. Bifurcation and Chaos, 1998, v. 8, No. 9, p. 1839-1842.
[23] A. Mögel *et al*. Chaotic wide band oscillator with delay line, in: Proc. 3rd Int. Workshop on Nonlinear Dynamics of Electronic Systems, NDES'95, Dublin, Ireland, p. 259-262.

# DISCLAIMER

Any opinions, findings and conclusions or recommendations expressed in this material are those of the authors and do not necessarily reflect the views of the European Office of Aerospace Research and Development, Air Force Office of Scientific Research, Air Force Research Laboratory.

Arūnas Tamaševičius, Habil. Dr.
Principal Investigator

# DECLARATION

The Contractor, Semiconductor Physics Institute, hereby declares that, to the best of its knowledge and belief, the technical data delivered herewith under Contract No. F61775-01-WE065 is complete, accurate, and complies with all requirements of the contract.

DATE: July 30, 2002
Name and Title of Authorized Official: Skaidra Bumelienė
Scientific secretary
of the Semiconductor Physics Institute

# STATEMENT

I certify that there were no subject inventions to declare as defined in FAR 52.227-13, during the performance of the Contract.

DATE: July 30, 2002
Name and Title of Authorized Official: Skaidra Bumelienė
Scientific secretary
of the Semiconductor Physics Institute